INTERACTIONS OF ORGANOPHOSPHORUS COMPOUNDS WITH ACETYLCHOLINESTERASE: A QM, QM/QM and QM/MM INVESTIGATION

J. B. Wright
U.S. Army SBCCOM, Natick Soldier Center, SS&TD
Natick, MA 01760

Margaret Hurley
U.S. Army Research Laboratory, CISD
Aberdeen Proving Ground, MD 21005

William E. White
U.S. Army Edgewood Chemical & Biological Center
Aberdeen Proving Ground –EA, MD 21010

Gerald Lushington
Molecular Graphics and Modeling Laboratory, University of Kansas
Lawrence, KS 66045

ABSTRACT

Nerve agents are the most toxic class of chemical warfare agents. They pose a major threat to DoD personnel and operations – not only from overt military attacks but also from terrorist activities and other low intensity conflicts. These compounds function by irreversibly inhibiting acetylcholinesterase (AChE), thus significantly interfering with human neural function. The molecular interactions that hold the enzyme in its optimal conformation and promote catalysis have never been elucidated. As a result, toxicity predictions of novel organophosphorus (OP) compounds and antidote effectiveness can only be made by extrapolations from closely related analogs. Theoretical calculations have been performed on this enzyme for several years; however, until our recent awards of two DoD HPC Challenge grants the lack of sufficient computing power placed severe limitations on the rigor of the method and the extent of the active site model. While prior calculations were restricted either to low levels of theory, or to truncated analogs containing only the amino acids in the active site, we have recently acquired the capacity for highly sophisticated simulations in which all relevant reactivity is treated at high levels of theory, and is effectively embedded in a lower level model capable of accounting for all important environment effects.

This investigation will provide highly accurate and reliable characterizations of the biochemical processes responsible for both activity and inhibition of novel OP compounds. It is expected that our results should prove relevant to toxicological endeavors within the medical and non-medical community alike.

1. INTRODUCTION

The enzyme AChE has been a topic of interest to theoreticians and experimentalists alike for a number of years. A large amount of this effort in the medical and academic communities has been in the course of investigating diseases such as Alzheimer's and myasthenia gravis. However, the enzyme has remained of key interest for military and civilian security personnel for the role it plays in nerve agent activity and inhibition. OP compounds such as nerve agents and insecticides are toxic chemicals that inhibit the function of AChE (Eto, 1974). Acetylcholine, a neurotransmitter, has an important role of transmitting electrical impulses across neuro-neuro or neuro-muscular junctions (synapses). Acetylcholine is released at a nerve end (axon end), travels across the synapse to the receptor site on the post-synaptic membrane and stimulates another neuron or muscle fiber. The active acetylcholine in the synaptic cleft is immediately hydrolyzed to inactive choline and acetate via the serine residue of AChE in a two-step process. In the transesterification step, the acetate moiety is transferred from the choline to a serine residue on the active site of the enzyme. In the second step, water hydrolyzes the acetylated serine to form acetic acid and regenerate the enzyme for subsequent acetylcholine catalysis (Figure 1) (Taylor and Brown, 1994).

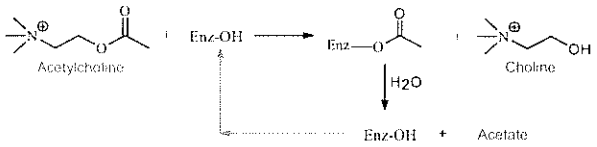

Figure 1. Schematic of: 1) transesterification of acetylcholine and 2) regeneration of AChE via hydrolysis.

As is the case for carbonyl esters, the serine anion is capable of attacking phosphorus esters and carbamates. Unfortunately, water does not have sufficient nucleophilic strength to hydrolyze the phosphylated or carbamalated serine. Thus, with these substrates, the enzyme active site becomes blocked leading to the uncontrolled accumulation of acetylcholine at the neuro-neuro and neuro-muscular junctions, causing a wide variety of life-threatening symptoms (Figure 2) (Heilbronn, 1993; (Schwartz, 1985).

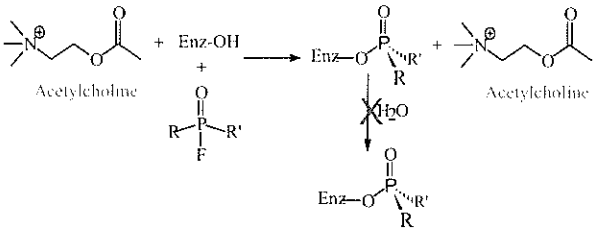

Figure 2. Schematic of the phosphorylation of AChE and the subsequent accumulation of acetylcholine.

A key feature of the enzyme active center is the catalytic triad, which consists of serine-200, histidine-440, and glutamate-327 (residue numbering according to *Torpedo Californica* AChE structure (Harel et al., 1996)). An important aspect of the catalysis is the facile formation of the nucleophilic serine anion. To form this anion, a proton is transferred from the hydroxyl group on Ser-200 to a nitrogen atom in the imidazole ring of His-440. Simultaneously, a proton is transferred from the other nitrogen in the ring to the carboxyl group on Glu-327. This proton transfer is expected to proceed concurrently with the nucleophilic attack on the carbonyl group of acetylcholine (or the phosphonyl group on Methyl Methylphosphonofluoridate as depicted in Figure 3). An important additional structural feature is the nearby oxyanion hole (Gly-118, Gly-119, and Ala-201 in the *Torpedo* numbering), which performs the function of stabilizing the negative charge developing on the anionic moiety of the ligand (Figure 3).

During the last half century, considerable empirical data has emerged regarding the substrate/activity relationships of AChE, rates of inhibition, and nucleophiles for removing the adducts, and a considerable body of literature pertaining to agent toxicity and

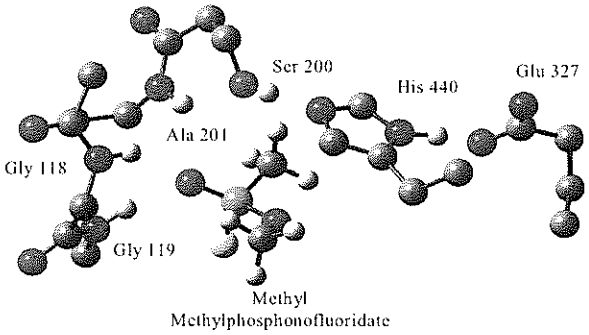

Figure 3. Significant residues of the active site of AChE (*Torpedo Californica*) with a generic OP compound, Methyl Methylphosphonofluoridate. For simplicity, only the significant protons are depicted. The catalytic triad consists of Ser-200, His-440, and Glu-327. The oxyanion hole consists of Gly-118, Gly-119, and Ala-201. The Ser-200 hydroxyl group is lined up opposite to the phosphinate fluoride. The phosphinyl group is coordinated in the oxyanion hole.

prophylaxis has evolved (Broomfield et al., 1999; (Doctor et al., 1999; (Millard et al., 1999; 2001). However, a detailed understanding of the mechanistic underpinnings and systematic anatomization of AChE inhibition, regeneration, and aging has remained elusive, in part due to the system size and complexity. Many early approaches entailed semi-empirical calculations on a truncated trypsin enzyme containing the active center and a few additional amino acids (Daggett et al., 1991). The main alternatives to semi-empirical methods have been the fully empirical techniques such as classical molecular dynamics (MD) and molecular mechanics (MM) wherein the entire protein may be studied, but at the expense of omitting explicit electronic structural effects that are fundamental to reliable prediction of chemical reactivity (Albaret et al., 1997; (Fuxreiter and Warshel, 1998).

Among the most important prior efforts in AChE activity modeling is that of Kovach et al., who employed a variety of techniques (including MM, MD and ab initio quantum chemical formalisms) to study AChE substrate binding and transition state structure (Bencsura et al., 1996). Via quantum chemical means, it was possible to determine a candidate structure for a prospective pentavalent transition state and develop a classical force field from those calculations. The pentavalent phosphonate was then placed inside the enzyme active site, and binding to the neighboring amino acid residues was studied. These latter studies were fundamentally limited, however, in that the absence of explicit electronic structural information in the classical model precluded a reliable simulation of bond breakage and activation energy prediction for the reaction. Additional formidable MD work on AChE has been performed by McCammon and coworkers to address complex structural issues involving solvation, the hypothetical "back door" to the

active site, and gating of the gorge (Shen et al., 2001; (Tai et al., 2001).

While classical MD work and truncated QM models of AChE have been the rule, a notable exception is the QM/MM work of Vasilyev (Vasilyev, 1994), who used a combination of PM3 and the OPLS force field to study protonation within the catalytic triad, as well as inhibition by a simple organophosphate P(F)(O)(NH_2)(CH_3). It is important to note that in this model only the catalytic triad side chains and the substrate were studied at the quantum level, and the surrounding enzyme environment was held fixed.

Similar enzyme processes have been the focus of theoretical studies performed with a variety of clever techniques to obviate the problems associated with inadequate computer power. Of particular interest is a recent QM/MM study of the catalytic mechanism for citrate synthase (Mulholland et al., 2000), which is relevant to the current effort as it involves the transfer of a methyl proton on acetyl CoA to asparate-375 and the possible protonation of the carbonyl oxygen by histidine-274. Also extremely relevant are the QM/MM studies of Topf et al. on the deacylation step of the serine protease elastase (Topf et al., 2001).

This paper represents initial results in an attempt to use QM, QM/QM and QM/MM methodologies to provide accurate and reliable characterization of model OP compound activity and inhibition of the AChE active site. Two methodologies, the ONIOM method (Dapprich et al., 1999) and the related SIMOMM method (Shoemaker et al., 1999), are used to study both bare AChE, and a series of systems involving model OP compounds. The roles of model size, force field, and methodology are examined, as well as the chemical structure of the catalytic triad (including the existence of the Short Strong Hydrogen Bond or SSHB), which are a vital aspect of the efficacy of the enzyme. The energetics, transition state formation, and the role of the oxyanion hole are being investigated.

2. METHODS

2.1 Codes

The IMOMM (and related) methodology of Morokuma was one of the early QM/MM implementations available to the non-specialist user (Maseras and Morokuma, 1995). A number of academic and commercial codes still rely on permutations of this algorithm. ONIOM calculations in this work have been performed using the Gaussian codes (Frisch et al., 1998). This work has been performed on several size models of the AChE active site, both with and without a model OP compound. In addition, these results have been augmented by calculations performed using the IMOMM-based SIMOMM method of Burggraf et al. as implemented in the GAMESS-US code (Schmidt et al., 1993). This implementation uses the Tinker package of Ponder et al. (Pappu et al., 1998) for the MM component. One of the major conceptual differences between ONIOM and SIMOMM lies in the treatment of atoms in the MM region that are directly bound to the QM region (which will be referred to here as "boundary atoms"), and in treatment of the atoms (typically hydrogens) added to the QM region to terminate dangling bonds. Boundary atoms in ONIOM represent a specific subset of the bulk region and are fixed during the optimization. In the SIMOMM method, boundary atoms are treated no differently than the rest of the MM region and are allowed to optimize in response to the MM gradient. Similarly, termination atoms in the QM region are fixed in the ONIOM method, yet optimized in SIMOMM in response to the QM gradient. It is the contention of the SIMOMM developers that this improves the calculation by removing user-defined constraints. Additional trivial differences arise in terms of available force fields, etc.

2.2 Enzymes/ Methodology

A number of reliable experimentally derived crystal structures for various forms of AChE are available. Crystal structures for both *Torpedo Californica* and *Mus Musculus* (1AMN and 1MAA) have been obtained from the RCSB databank and have been used to obtain starting structures. Due to the shear size of the enzyme (over 5000 heavy atoms), calculations have been performed using the "Ribbon Methodology." This methodology consists of collecting all the enzyme atoms surrounding the active site serine hydroxyl group out to a predefined distance (Figure 4A) thus eliminating the need to truncate the active site residues. All atoms outside of the sphere are eliminated. This will leave segments of the overall enzyme ribbon inside the sphere (Figure 4B). The ends of each ribbon segment are locked in space. This "Ribbon Methodology" will permit structural relaxation of the active site atoms and flexible response to the insertion of model OP compounds. In other words, this methodology

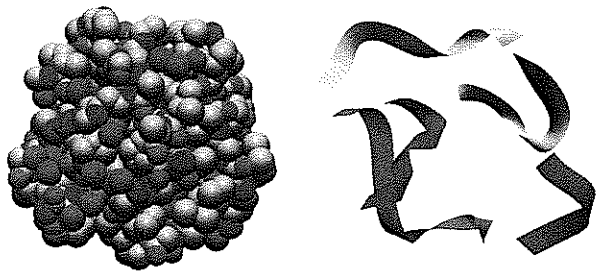

Figure 4. A) CPK model of a sphere of atoms with a radius of 10 angstroms from the Ser-200 hydroxyl group in the active site. B) The corresponding ribbon structure showing the five ribbon segments whose ends terminate on the sphere surface.

will allow enough flexibility in the active site to investigate the chemistry but retains sufficient rigidity such that the active site does not fall apart. The main consequence of this flexible methodology is the elimination of the use of expensive solvation methods since a predefined layer of enzyme atoms surrounds the active site chemistry being investigated.

Various model sizes have been investigated, ranging from a small model (containing only the active site residues plus a model OP compound), to an intermediate model (containing the active site residues, the oxyanion hole residues and the model OP compound), to two larger models (comprised of all residues which at least partially reside within a 7 or 10 angstrom radius of the active site, augmented with further residues to preserve natural ribbon contiguity). Methyl groups were added to terminal residue backbone nitrogens to truncate the chain. The Rasmol software was used to carve the model residues from the PDB file, and hydrogens were added to the structures using the protonate facility of AMBER. For the small and intermediate models, constraints were placed on terminal carbon atoms for each chain to keep the model intact. No optimization constraints were used on the 7 and 10-angstrom models. Concurrent work is underway to study the energetics of model OP compound hydrolysis in water, as well as model OP compound-enzyme interactions including explicit waters, which will be reported elsewhere.

3 RESULTS AND DISCUSSION

3.1 Bare Enzyme

NMR studies of the AChE active site structure suggest strong coupling between residues of the SER→HIS→GLU catalytic triad in the form of strong hydrogen bonding interactions. This H-bonded coupling is believed to be an essential factor in the proton transfer processes that enhance the catalytic nucleophilicity of such enzymes (Viragh et al., 2000). Specifically, the serine hydroxyl hydrogen is believed to experience a strong electrostatic attraction by a nitrogen on the nearby histidine ring. This interaction is stabilized by a short strong H-bond (SSHB) (alternatively known as a low barrier hydrogen bond or LBHB) between a nitrogenic proton on the histidine ring and the neighboring unprotonated glutamic acid residue – an arrangement for which proton NMR studies have predicted an $O_{GLU} - N_{HIS}$ SSHB distance of 2.64 ± 0.04Å (Viragh et al., 2000).

A series of QM/MM calculations were performed on the 7 and 10-angstrom bare enzyme models of *Mus Musculus* AChE (Bourne et al., 1999) using both the ONIOM and SIMOMM codes without constraints. Various levels of theory for the QM portion and various force fields for the MM portion were investigated. Difficulties arose for all cases except the ONIOM 7Å model with the Universal Force field (UFF) and the SIMOMM 10Å model with the AMBER force field. In these two later models, the proper alignments of the catalytic triad residues were observed. The ONIOM 7Å AChE (*Mus Musculas*) model using the B3LYP/3-21G** level of theory for the QM portion and the UFF force field for the MM portion with the proper catalytic triad alignment is depicted in Figure 5.

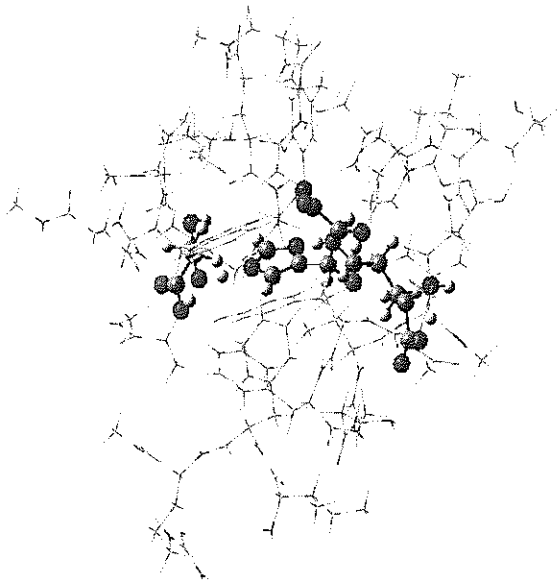

Figure 5. A 7Å AChE (*Mus Musculas*) example. The QM (Ball and stick) portion contains the catalytic triad residues calculated at the B3LYP/3-21G** level of theory. The MM (wire) portion, which surrounds the catalytic triad, is calculated using the UFF force field. Note the proper alignment of the catalytic triad. There are 254 heavy atoms plus 250 hydrogens in this example.

In general, the effects of theory level and basis set size for the QM portion are quite minor for both the ONIOM 7Å and SIMOMM 10Å cases. The ONIOM 7Å model consistently shows a minimum energy triad protonation state of Ser^0-His^--Glu^0, where the His-H_δ has effectively transferred to the Glu, while the Ser-H does not transfer to the His. The SIMOMM 10Å model shows more sensitivity to basis set size in that calculations performed with the high layer at RHF STO-3G and RHF 3-21G show a minimum energy state of Ser^0-His^0-Glu^-. Calculations performed with the high layer at RHF 6-31G and 6-31G(d) converge to a protonation state of Ser^0-His^--Glu^0. In this series of results, the AMBER force field has largely proven problematic. However, both methodologies do yield results with excellent alignment of the catalytic triad, and the ONIOM models have successfully reproduced the Short Strong Hydrogen Bond (SSHB) seen experimentally.

3.2 OP compound / Enzyme Calculations

Initial studies to locate transition states (TS's) included looking at the bare catalytic triad of AChE with Methyl Methylphosphonofluoridate, using only QM with G98. Two levels of theory, HF/6-31G(d) and B3LYP/6-31G(d,p), were investigated. The TS's for both levels of theory are depicted in Figure 6. The terminal methyl carbon atoms for serine, histidine and glutamate were locked in space while the other remaining atoms were allowed to fully optimize. In the HF/6-31G(d) level of theory, the main contributor to the imaginary frequency is the bond formation between the phosphorous atom and the O_{SER} with minor contribution to the movement of the SER-200 proton moving to the N_{1HS} (Figure 6A). This TS is dubbed a late TS due to the fact that the proton between the O_{GLU}-N_{1HS} has already formed a bond to the Glu-327 with a bond length of 0.98Å. It is also important to point out that there is no displacement of the proton between His-440→Glu-327 corresponding to the imaginary frequency in the HF level of theory. The transition state barrier for this reaction is quite high at 26.43 kcal/mol. In the B3LYP/6-31G(d) level of theory, the main contributor to the negative frequency is the displacement of the SER-200 proton moving to the His-440 nitrogen (Figure 6B). At the same time, there are two minor contributions to the imaginary frequency, which include the phosphorus- O_{SER} bond formation and the movement of the proton between the SSHB O_{GLU}-N_{1HS}. The B3LYP level of theory is considered an earlier TS when compared to the HF level. The distance for the O_{GLU}-N_{1HS} SSHB in the HF and B3LYP levels are 2.76 and 2.58Å, respectively (Figure 6A and 6B). The B3LYP level of theory more accurately shows the simultaneous proton transfers in the catalytic triad and correlates to the empirical SSHB bond distances, as well as demonstrating a significant lowering of the TS barrier to 15.27 kcal/mol using the B3LYP/6-31G(d) level of theory.

With the TS's found in the bare minimum catalytic-triad calculations, the ONIOM QM/QM methodology was then used to map out energetics of the phosphorylation reaction. First, an ONIOM=(HF/6-31G(d):HF/STO-3G) calculation was performed where the terminal methyl group of Glu-327 was calculated using the STO-3G basis set and all other atoms were calculated using the 6-31G(d) basis set (not depicted). As above, all terminal carbon atoms were frozen in space. The displacement of the TS imaginary frequency was identical to the QM HF level mentioned previously with the major contributor being the phosphorous-O_{SER} bond formation. This produced a 26.40 kcal/mol reaction barrier that is comparable to the QM HF level above and to a rough 30 kcal/mol barrier found in related calculations of phosphonate hydrolysis in aqueous solution (to be reported elsewhere).

A second set of calculations was then performed in which the reactant, TS and product minima were located using the ONIOM=(B3LYP/6-31G(d,p):B3LYP/3-21G**) levels of theory where the terminal ethyl group of Glu-327 formed the lower layer and all other atoms formed the higher layer (Figure 7). The displacement of the TS imaginary frequency was identical to the QM DFT calculation discussed in the previous paragraph with the major contributor being the displacement of the Ser-200 proton moving to the His-440 nitrogen. At the same time, there are two minor contributions to the imaginary frequency, which include the phosphorus-O_{SER} bond formation and the movement of the proton between the O_{GLU}-N_{1HS} SSHB. There is a 15.18 kcal/mol reaction barrier that is approximately half of the rough 30 kcal/mol barrier found in related calculations of phosphonate hydrolysis in aqueous solution (to be reported elsewhere). The proper hydrogen bond scheme is obvious from the structures and an SSHB of 2.59Å is seen in both the reactant and product with a shorter SSHB of 2.52Å in the TS.

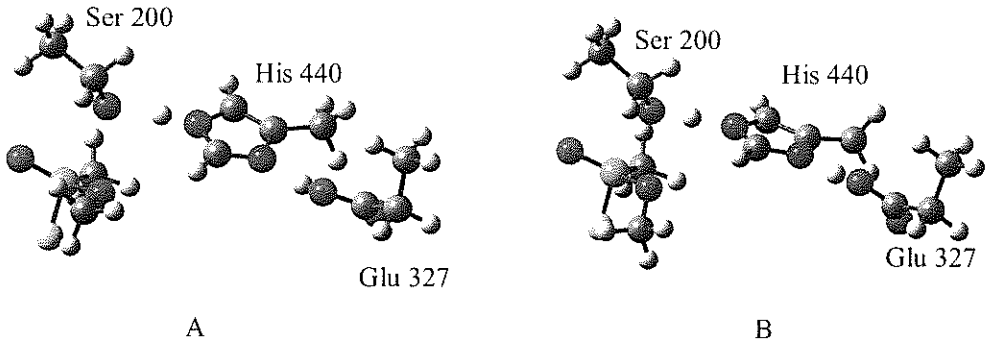

Figure 6. The TS's of the AChE (*Torpedo Californica*) catalytic triad reacting with Methyl Methylphosphonofluoridate at the A) HF/6-31G(d) and B) B3LYP/6-31G(d,p) levels of theory.

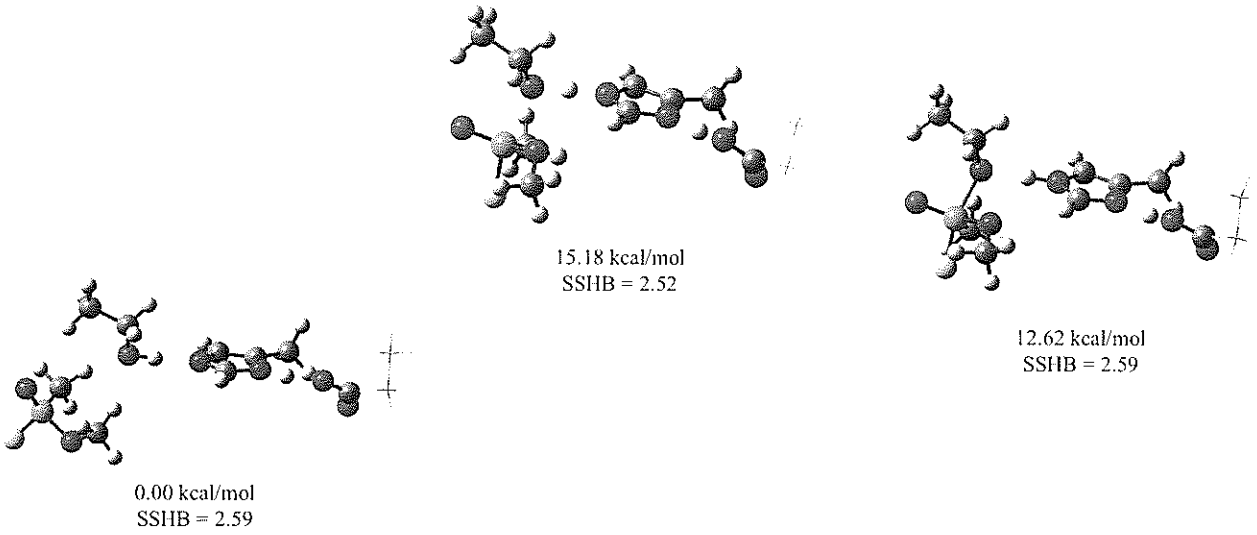

Figure 7. The reactant, TS, and product of the AChE (*Torpedo Californica*) catalytic triad reacting with Methyl Methylphosphonofluoridate using the QM/QM (B3LYP/6-31G(d,p):B3LYP/3-21G**) levels of theory. The relative energies in kcal/mol and SSHB distances in angstroms are also depicted.

Additional residues beside the catalytic triad are postulated to play a role in the phosphorylation reaction. Figure 8 depicts the reactant and product of an ONIOM=(B3LYP/6-31G(d,p):B3LYP/STO-3G) QM/QM calculation of the *Torpedo Californica* active site structure, which includes the oxyanion hole (Gly-118, Gly-119 and Ala-201). It is important to stress that the OP compound is free to move without constraints. However, as depicted in Figure 8, the phosphonyl bond of the reactant (and product) coordinates in the oxyanion hole (3 hydrogens) with the fluorine atom *anti* to the O_{SER}. The SSHB distance in the reactant and product is 2.65 and 2.63Å, respectively. While it is obvious from the reactant structure that the OP compound orients comfortably into the oxyanion hole before binding to the active site (and properly coordinates with the amide groups of the oxyanion hole backbone), the interaction is still stronger in the product structure. Distances between the substrate oxygen and Gly-118, Gly-119, and Ala-201 amide nitrogens in the product state are ~2.5Å with a roughly linear H-bond angle (~168-175). Comparison of calculated charges between the product and reactant state show the substrate oxygen to have drawn negative charge in the product state relative to the reactant state, as expected. This important electrostatic stabilization bespeaks the necessity of treating the oxyanion hole residues quantum mechanically. The stereosensitivity of the OP compound-AChE interactions has been demonstrated experimentally (Ordentlich et al., 1999), and we have chosen here ostensibly the most reactive forms of the model OP compounds. Investigations of reactions involving different stereoisomers, presentation of different faces of the model OP compound to the serine residues (and thus affecting orientation into the oxyanion hole and/or steric effects), and steric effects introduced by substitution of branched alkyl and alkoxy groups are currently under investigation and will be reported elsewhere.

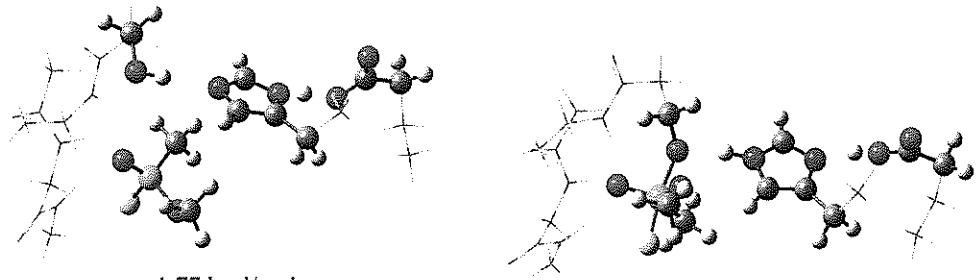

Figure 8. Reactant and product for the phosphonylation of the active site with the presence of the oxyanion hole (Gly-118, Gly-119 and Ala-201). QM/QM calculation using the ONIOM=(B3LYP/6-31G(d,p):B3LYP/STO-3G) levels of theory.

All reactions discussed to this point have shown the product with the fluorine-leaving group still attached to the phosphorus atom. This trigonal-bipyramidal intermediate would then lose the fluoride atom via the participation of solvent molecules to produce a tetrahedral product. Previous calculations attempting to map out the energetics of this fluoride loss with the use of water and hydronium molecules on the same side of the fluorine (*anti* to the F-P-O_{SER} angle) were unsuccessful. However, a unique TS through the participation of an ammonium ion has been located (Figure 9). This is a QM B3LYP/6-31G(d,p) calculation and as with previous calculation the terminal methyl groups are locked in space. This TS not only has the simultaneous dual catalytic triad proton transfer with the P-O_{SER} bond formation, but also has the fluoride departure (P-F bond breakage) simultaneous with the F-NH_4 bond formation. This results in a TS with eight bonds being made/broken simultaneously correlating to one imaginary frequency. Another important aspect of this TS is the elimination of the trigonal-bipyramidal intermediate which correlates well with additional OP solvation calculations currently underway. Preliminary results mapping out the energetics of this reaction show the tetrahedral product is 68 kcal/mol below the TS, thus showing the importance of the fluoride departure. The activation energy is currently under investigation.

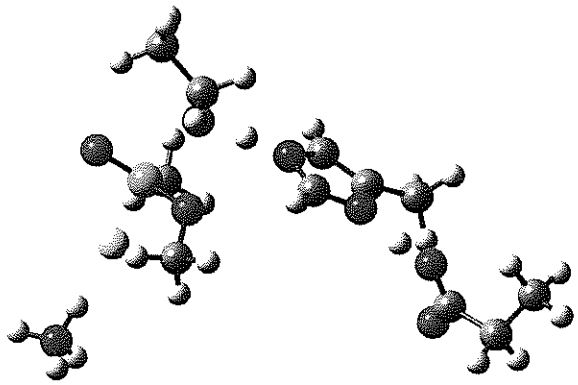

Figure 9. A QM B3LYP/6-31G(d,p) TS with the removal of fluorine via the participation of an ammonium ion.

Other calculations have looked at the participation of a hydronium molecule and a hydronium molecule associated with a water molecule wrapped in a 14 and 16-membered ring configuration. These TS's (named Anaconda I and II, respectively), show the fluorine-coordinated solvent molecules wrapping around and coordinating with the O_{GLU} of the catalytic triad creating electron flow through a 14 or 16-memberd ring. These unique TS's show the importance of solvent molecule participation in the overall scheme (Anaconda II is depicted in Figure 10).

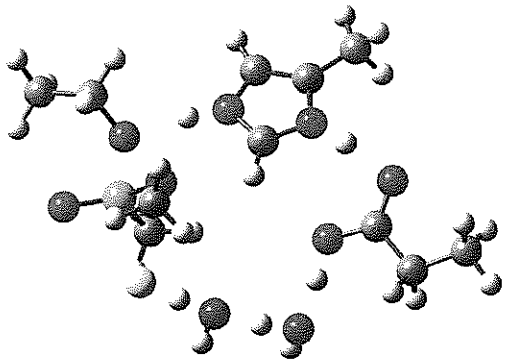

Figure 10. Anaconda II: A QM B3LYP/6-31G(d,p) TS with the removal of fluorine via the participation of hydronium and water molecules. Basically, a 16-membered ring with 12 simultaneous bonds being made/broken.

CONCLUSIONS

This study represents the initial phase of a project devoted to application of a variety of theoretical methods to investigate reactions of model organophosphorus compounds in the active site of AChE. Mixed QM/MM methods have been used to estimate the sensitivity of the catalytic triad of the bare enzyme to details of the model and we have achieved insight into the reactions of model OP compound species with the AChE active site. Without high-level electronic structure methods, these calculations cannot accurately predict empirical results. The location of transition states, which is unarguably the most challenging aspect of computational endeavors, has produced novel solvent-participation mechanisms with as many as twelve simultaneous bonds being made/broken in a sixteen-membered ring correlating to one imaginary frequency.

Our results, which shed light on the underpinnings of the catalytic mechanism (to include the participation of solvent molecules), also produce data that is in agreement with empirical data. We expect future work to prove equally beneficial by exploring key structural features leading to reversible and irreversible binding to the enzyme, thereby obtaining definitive results on phenomena not readily accessible by traditional chemical or spectroscopic methods.

ACKNOWLEDGMENTS

This work was supported in part by a grant of computer time from the DOD High Performance Computing Modernization Program at ARL, ASC, and ERDC MSRCs. Partial funding has been provided through a DoD JSTPCBD proposal.

REFERENCES

Albaret, C., Lacoutiere, S., Ashman, W.P., Froment, D. and Fortier, P.-L., 1997. Molecular Mechanic Study of Nerve Agent O-ethyl S-[2-(diisopropylamino)ethyl]methylphosphonothioate (VX) Bound to the Active Site of *Torpedo californica* Acetylcholinesterase. Proteins: Structure, Function, and Genetics, 28: 543-555.

Bencsura, A., Enyedy, I.Y. and Kovach, I.M., 1996. Probing the Active Site of Acetylcholinesterase by Molecular Dynamics of Its Phosphonate Ester Adducts. J. Am. Chem. Soc., 118: 8531-8541.

Bourne, Y., Taylor, P., Bougis, P.E. and Marchot, P., 1999. Crystal Structure of Mouse Acetylcholinestease. A Peripheral Site - Occluding Loop in a Tetrameric Assemble. J. Biol. Chem, 274: 2963-2970.

Broomfield, C.A., Lockridge, O. and Millard, C.B., 1999. Protein engineering of a human enzyme that hydrolyzes V and G nerve agents: design, construction and characterization. Chem. Biol. Interact., 119-120: 413-418.

Daggett, V., Schroder, S. and Kollman, P., 1991. Catalytic Pathway of Serine Proteases: Classical and Quantum Mechanical Calculations. J. Am. Chem. Soc., 113: 8926-8935.

Dapprich, S., Komaromi, I., Byun, K.S., Morokuma, K. and Frisch, M.J., 1999. A New ONIOM Implementation in Gaussian 98. Part I. The Calculation of Energies, Gradients, Vibrational Frequencies and Electric Field Derivatives. J. Mol. Struct. (THEOCHEM), 461: 1-21 and references therein.

Doctor, B.P., Taylor, P., Quinn, D.M., Rotundo, R.L. and Gentry, M.K., 1999. Structure and Function of Cholinesterases and Related Proteins. Kluwer Academic/Plenum Publishers, Dortrecht and references therein.

Eto, M., 1974. Organophosphorus Pesticides: Organic and Biological Chemistry. CRC Press, Boca Raton, FL.

Frisch MJ, Trucks GW, Schlegel HB, Scuseria GE, Robb MA, Cheeseman JR, Zakrzewski VG, Montgomery JA, Stratmann RE, Burant JC, Dapprich S, Millam JM, Daniels AD, Kudin KN, Strain MC, Farkas O, Tomasi J, Barone V, Cossi M, Cammi R, Mennucci B, Pomelli C, Adamo C, Clifford S, Ochterski J, Petersson GA, Ayala PY, Cui Q, Morokuma K, Malick DK, Rabuck AD, Raghavachari K, Foresman JB, Cioslowski J, Ortiz JV, Stefanov BB, Liu G, Liashenko A, Piskorz P, Komaromi I, Gomperts R, Martin RL, Fox DJ, Keith T, Al-Laham MA, Peng CY, Nanayakkara A, Gonzalez C, Challacombe M, Gill PMW, Johnson BG, Chen W, Wong MW, Andres JL, Gonzalez C, M. Head-Gordon, Replogle ES, Pople JA, (*Gaussian 98* (Revision A.7), Gaussian, Inc., Pittsburgh, PA, 1998).

Fuxreiter, M. and Warshel, A., 1998. Origin of the Catalytic Power of Acetylcholinesterase: Computer Simulation Studies. J. Am. Chem. Soc., 120: 183-194.

Harel, M., Quinn, D.M., Nair, H.K., Silman, I. and Sussman, J.L., 1996. The X-ray structure of a transition state analog complex reveals the molecular origins of the catalytic power and substrate specificity of acetylcholinesterase. J. Am. Chem Soc., 118: 2340-2346.

Heilbronn, E., 1993. Molecular Biology of Cholinesterases: A Background and an Introduction. In: A.C. Cuello (Editor), Cholinergic Function and Dysfunction. Cholinergic Function and Dysfunction. Elsevier, NY, pp. 133-138.

Maseras, F. and Morokuma, K., 1995. J. Comput. Chem., 16: 1170-1180.

Millard, C.B. et al., 1999. Crystal structures of aged phosphonylated acetylcholinesterase: nerve agent reation products at the atomic level. Biochemistry, 38(22): 7032-7039.

Mulholland, A.J., Lyne, P.D. and Karplus, M., 2000. Ab initio QM/MM Study of the Citrate Synthase Mechanism. J. Am. Chem. Soc., 122: 534-535.

Ordentlich, A. et al., 1999. Exploring the Active Center of Human Acetylcholinesterase with Stereomers of an Organophosphorus Inhibitor with Two Chiral Centers. Biochemistry, 38(12): 3055-3066.

Pappu, R.V., Hart, R.K. and Ponder, J.W., 1998. J. Phys. Chem. B, 102: 9725-9744 and references therein.

Schmidt, M.W. et al., 1993. J. Comput. Chem., 14: 1347-1363.

Schwartz, J.H., 1985. Molecular Aspects of Postsynaptic Receptors. In: E.R. Kandel and J.H. Schwartz (Editors), Principles of Neural Science. Principles of Neutral Science. Elsevier, NY, pp. 159-168.

Shen, T.Y., Tai, K. and McCammon, J.A., 2001. Phys. Rev. E., 63: 041902 and references therein.

Shoemaker, J., Burggraf, L.W. and Gordon, M.S., 1999. SIMOMM: An Integrated Molecular Orbital/Molecular Mechanics Optimization Scheme for Surfaces. J. Phys. Chem. A, 103: 3245-3251.

Somani, S.M. and Romano, J.A.J., 2001. Chemical Warfare Agents: Toxicity at Low Levels. CRC Press, Boca Raton, FL and references therein.

Tai, K., Shen, T., Borjesson, U., Philippopoulos, M. and McCammon, J.A., 2001. Biophys. J., 81: 715-724.

Taylor, P. and Brown, J.H., 1994. Acetylcholine. In: G.J. Siegel, B.W. Agranoff, R.W. Abbers and P.B. Molinoff (Editors), Basic Neurochemistry: Molecular, Cellular, and Medical Aspects. Basic Neurochemistry: Molecular, Cellular, and Medical Aspects. Raven Press Ltd., NY, pp. 231-260.

Topf, M., Varnai, P. and Richards, W.G., 2001. Theor. Chem. Act., 106: 146-151.

Vasilyev, V.V., 1994. J. Mol. Struct (THEOCHEM), 304: 129-141.

Viragh, C. et al., 2000. NMR Evidence for a Short, Strong Hydrogen Bond at the Active Site of a Cholinesterase. Biochemistry, 39: 16200-16205.